J Mater Sci: Mater Med (2009) 20:2305–2316
DOI 10.1007/s10856-009-3800-7

Specific biofunctional performances of the hydroxyapatite–sodium maleate copolymer hybrid coating nanostructures evaluated by in vitro studies

L. E. Sima · A. Filimon · R. M. Piticescu · G. C. Chitanu · D. M. Suflet · M. Miroiu · G. Socol · I. N. Mihailescu · J. Neamtu · G. Negroiu

Received: 15 December 2008 / Accepted: 4 June 2009 / Published online: 20 June 2009

Abstract The nanohybrid structures consisting of hydroxyapatite (HA) and sodium maleate-vinyl acetate copolymer (MP) deposited by Matrix Assisted Pulsed Laser Evaporation (MAPLE) technique on Ti surfaces were investigated for specific biological qualities required in bone implantology. The data from in vitro studies demonstrated that human primary osteoblasts (OBs) firmly adhered to Ti coated with HA–MP as indicated by cytoskeleton and vinculin dynamics. OBs spread onto biomaterial surface and formed groups of cells which during their biosynthetic activity expressed OB phenotype specific markers (collagen and non-collagenous proteins) and underwent controlled proliferation.

L. E. Sima · A. Filimon · G. Negroiu (✉)
Institute of Biochemistry, Romanian Academy, Splaiul Independentei 296, Bucharest 060031, Romania
e-mail: gnegroiu@biochim.ro; gabrielanegroiu@yahoo.com

R. M. Piticescu
National R&D Institute for Non-ferrous and Rare Metals, 102 Biruintei Blvd., Pantelimon-Ilfov, Romania

G. C. Chitanu · D. M. Suflet
"Petru Poni", Institute of Macromolecular Chemistry, Aleea Gr. Ghica Voda 41A, Iasi 700487, Romania

M. Miroiu · G. Socol · I. N. Mihailescu
National R&D Institute for Lasers Plasma and Radiation Physics, 409 Atomistilor Str., Magurele – Ilfov, Romania

J. Neamtu
University of Medicine and Pharmacy, Craiova, Romania

1 Introduction

The necessity to correct or replace injured tissues or organs of the human body has led to tremendous production of various implantable devices [1]. Nevertheless, despite the excellent mechanical or physico-chemical performances, a material destined to function in living environment has to be biocompatible. The general concept according to which a non cytotoxic device was assumed as *biocompatible* has been revised due to unexpected adverse reactions triggered by long term contact of different biomaterials with living organism [2–4]. An ideal biomaterial has to perform as many functions as possible of the replaced body part and must not alert the host defense mechanisms. Thus, numerous in vitro, followed by in vivo tests are undertaken by the newly developed biomaterials, in order to be eventually recommended for implantation in humans. For ethical and practical considerations the in vitro testing had to be extended from simple screening for cytotoxicity to specific and appropriate assays more related to the purpose for which these devices were created [5]. There is a great variety of in vitro parameters as cell viability [6, 7], adhesion [8], biosynthetic activity [9], proliferation [10, 11] apoptosis or necrosis [12, 13] which are estimative for the physiological state of cells grown in contact with biomaterials. In addition, specific biomarkers which monitor the biomaterial capacity to induce transformation [14–16] or differentiation [17] are assessed during the in vitro tests.

The biomaterials destined to dental or orthopedic use are expected to induce osteointegration, namely to allow bone cells to firmly adhere and normally function on their surfaces. The complex physiology of bone cells enables them with the capacity to synthesize the major components of their extracellular matrix (ECM), including type I collagen which forms the backbone of matrix and accounts for 90%

of the organic component and non collagenous glycoproteins. These are bound to the matrix and grouped as adhesion proteins (osteopontin, fibronectin, thrompospondin), calcium binding proteins (osteonectin, bone sialoprotein) and proteins involved in mineralization (osteocalcin). Bone tissue also contains complex molecules of inorganic elements (65%), such as hydroxyapatite (HA)-$Ca_{10}(PO_4)(OH)_2$, which confers strength and hardness to bone tissue. The correct assembly of bone ECM represents the critical factor responsible for the remarkable resistance of this tissue to mechanical stress and makes it the storehouse for the body calcium, magnesium and phosphorus.

It has been demonstrated that local adverse reactions caused by metallic implants originate from the release of metal ions as a result of corrosion [18–20]. By coating metal implants with ceramic-like structures based on calcium phosphate containing materials that mimic natural HA, the cytotoxicity or inflammatory reactions of surrounding tissues in response to metal ion leakage were significantly attenuated [21].

New combinations of HA with different compounds are continuously created and screened for their physicochemical and biological properties in order to select stable and well tolerated coating surfaces [22–26]. The great diversity of bone implants based on Ti and Ti alloys comes also from their deposition procedures. For tissue engineering, successful deposition of uniform adherent and functional layers of organic materials such as gas sensing biopolymers, collagen nanofibrils, fibrinogen and other proteins have been performed by MAPLE technique [27–32]. This advanced pulsed laser technique has been developed during the last decade, to produce a *protected* accurate transfer of organic and polymeric materials in form of thin films, due to a cryogenic approach [27, 28]. The material subjected to the laser irradiation is a frozen composite, obtained by the dissolution of the material (up to 5 wt%) in a volatile solvent highly absorbing the laser wavelength. The laser pulse intensity is adjusted to avoid the damage of the organic material. The structural and functional fidelity is preserved by inducing a non-direct laser-material interaction in a vacuum chamber. Due to the low concentration of organic molecules in the frozen target, the laser photons preponderantly interact with the matrix (the solvent), which is vaporized. The complex molecules are released undamaged and moved toward the substrate by collisions with the other molecules. In time, the volatile solvent is pumped away. As its precursor, Pulsed Laser Deposition (PLD), MAPLE is a layer-by-layer deposition method, which can deposit thin films with or without dopants and may also be applied with masks, in order to induce a controlled distribution of the local structure parameters by the nature and type of the coating.

The combination between HA and sodium maleate copolymers represents a relatively new class of hybrid structures destined to the coating of metallic surfaces of biomaterial devices used in dental and bone implantology. This association was based on previously demonstrated properties of maleic anhydride copolymers as modulators of size and shape of crystals and inhibitors of crystal growth [33, 34]. Recent studies revealed the specific effect of maleic anhydride copolymers on the phase separation of HA at room temperature as well as their performances as additives in preparation of HA by hydrothermal method, when nanosized particles of polymer-HA composites were obtained [35, 36].

The nanohybrids of HA with sodium maleate-vinyl acetate copolymer (MP) deposited on Ti surfaces by MAPLE technique were tested for the first time for their biocompatibility in our previous study [37]. The experimental data established that HA–MP coatings were not cytotoxic and sustained dermal fibroblast and mesenchymal stem cell adhesion, growth and proliferation.

The purpose of the present work was to investigate the HA–MP coating by additional in vitro tests in order to validate their specific functional properties, which would qualify them for being used in vivo on animal models. The experiments were performed using primary osteoblasts obtained by differentiation from bone marrow mesenchymal stem cells. HA–MP nanocomposites structure deposited onto Ti surfaces by MAPLE were comparatively analyzed with Ti coated with HA or MP alone and with standard borosilicate cover glass. The expression of cell adhesion and proliferation markers, cytoskeleton dynamics as well as markers of OB specific phenotype was analyzed by immunofluorescence microscopy. The CFSE (carboxyfluorescein succinimidyl ester) test was used to quantitatively assess the proliferation of OBs grown in direct contact with the biomaterial coated surfaces. Our data showed that HA–MP deposited by MAPLE ensures proper osteoblast adhesion, functionality and proliferation and would represent a better coating alternative for Ti surfaces than HA or MP alone.

2 Materials and methods

2.1 Ti coated with hybrid nanocomposites of HA–sodium maleate copolymer (Ti–HA–MP)

The copolymer used as organic partner in the fabrication of hybrid composites was the 1:1 alternating copolymer sodium maleate (NaM)–vinyl acetate (VA) which was obtained from the corresponding maleic anhydride (MA)–VA copolymer. The parent copolymer was synthesized and characterized as previously described [38, 39].

The copolymer NaM–VA was prepared by mild hydrolysis with diluted aqueous NaOH solution at room temperature for 24 h and carefully purified by dia-filtration until the filtrate conductivity was lower than 20 lS/cm. The copolymer NaM–VA was recovered by freeze drying and further referred as MP copolymer.

Hybrid nanocomposites (HA–MP) used for Ti coating were obtained starting from soluble salts of calcium, phosphorous and MP copolymer by hydrothermal method described in detail elsewhere [35]. Nanocomposites consisting of 1% HA–MP powder containing 20% copolymer were deposited onto 12 mm disk-shaped Ti surfaces by MAPLE technique. A KrF excimer laser source ($\lambda = 248$ nm, $\tau \leq 25$ ns) was used while the following MAPLE deposition parameters have been applied: substrate temperature 30°C, target–substrate separation distance of 4 cm, pressure inside the deposition chamber of 5.33 Pa, pulses of 0.54 J/cm^2 incident laser fluence, succeeding at a repetition rate of 10 Hz and 25,000 subsequent laser pulses for the deposition of one structure of about 300 nm thickness (as monitored by profilometry). Alternatively, Ti coated with HA (Ti–HA) or with copolymer (Ti–MP) structures of the same thickness have been prepared by MAPLE and investigated together with Ti–HA–MP samples.

Prior biological tests samples were sterilized two times for 90 min at 110°C each.

2.2 Cell culture

All experiments were performed with human primary osteoblasts obtained in our laboratory by differentiation from human mesenchymal stem cells (HMSC). HMSC were isolated from bone marrow and cultured in the expansion medium (DMEM, 15% FCS) (Biochrom AG) as described [37]. The MSC phenotype was validated by flow cytometry analysis (FACSCalibur from BD Biosciences) when cells were found positive for CD13, 29, 90 and negative for CD14, 34, 45. In order to obtain primary osteoblasts, HMSC at passage 2 were further cultured in α-MEM (Biochrom AG) supplemented with osteogenic factors: 82 μg/ml ascorbic acid, 100 nM dexametazone and 10 mM β-glycerophosphate. At the end point of differentiation (21 days) cells were tested for the expression of several proteins specifically produced by bone cell phenotype. These cells representing primary osteoblasts were used for further experiments with composites-coated Ti and were referred in text as OBs.

2.3 Microscopy

HMSC (5.0×10^3 cells) were cultured in osteogenic medium onto standard borosilicate cover glass (12 mm diameter) (Thermo Scientific) for the indicated time periods and observed by light microscopy (Nikon Eclipse E 600 microscope) using DIC optics. OBs or HMSC grown in standard conditions or in direct contact with Ti–HA, Ti–MP or Ti–HA–MP were analyzed for actin or protein expression of adhesion, proliferation and OB phenotype markers by immunofluorescence as previously described [37]. Fixed and permeabilized cells were incubated with: mouse anti-collagen type I (1:50), rabbit anti-osteocalcin (1:100), rabbit anti-osteonectin (1:1000), all from Chemicon International; mouse anti-bone morphogenetic protein-2 (1:200) (Santa Cruz Biotechnology), mouse anti-osteopontin (1:100) (Novocastra), mouse anti-vinculin (1:150) (Sigma), mouse anti-FAK (1:200) (BD Transduction Labs), mouse anti-Ki67 (1:100) (Zymed). Rabbit antibodies were detected with either goat-anti-rabbit Alexa Fluor 594 (red) or 488 (green) and mouse antibodies were detected with either goat anti-mouse labeled with Alexa Fluor 594 or 488; actin filaments were stained following 30 min incubation at RT with Alexa Fluor 594 phalloidin (1:50) (Invitrogen). Samples were mounted in ProLong Gold antifade reagent with DAPI (Invitrogen) to visualize nuclei and analyzed with a Nikon Eclipse E 600 fluorescence microscope; all images were processed using Adobe Photoshop 7.0 software.

2.4 Proliferation assay

OB proliferation was determined by flow cytometry using CellTrace CFSE Cell Proliferation Kit (Molecular Probes). OBs (3×10^3 cells) were labelled day 0 with CFSE fluorescent solution (as suggested by manufacturer) and seeded on the surfaces of borosilicate standard material (control sample) or on Ti–HA, Ti–MP and Ti–HA–MP materials. All biomaterials were analyzed in duplicates. After 6 days in culture cells were harvested and acquired by flow cytometry to register emission on the FL-1 channel with a FACSCalibur. The fluorescence of mother cell will be inherited by daughter cells, moving to lower values after each cell division and is not transferred to adjacent cells in a population. The data were analyzed using CellQuest Pro software and the proliferative cell population was thus assayed as the one with low levels of fluorescence signal.

3 Results

3.1 Immunocytochemical characterization of primary osteoblasts differentiated from mesenchymal stem cells

Cell morphology and cytoskeleton (actin-ACT) dynamics during HMSC differentiation period were observed (Fig. 1).

HMSC cells at day 1 of incubation with osteogenic medium had typical fibroblast-like morphology with long, thick, parallel ACT filaments. At day 7 cell morphology was changed displaying extended dendrites and prominent nuclei; after 14 days cells became more adherent and flatten; cell body occupied large areas and therefore cell contour was hardly detected; mineralization foci (nodules) appeared as fine dots in the intercellular space. After 21 days in culture cells interconnect with each other forming a syncytium; cytoskeleton ACT filaments staining demonstrate a distinct morphology of those cells compared with the originating MSC phenotype (Fig. 1, Actin, HMSC-day1, versus HMSC-day 21). In order to validate the OB phenotype, the expression and subcellular localization of

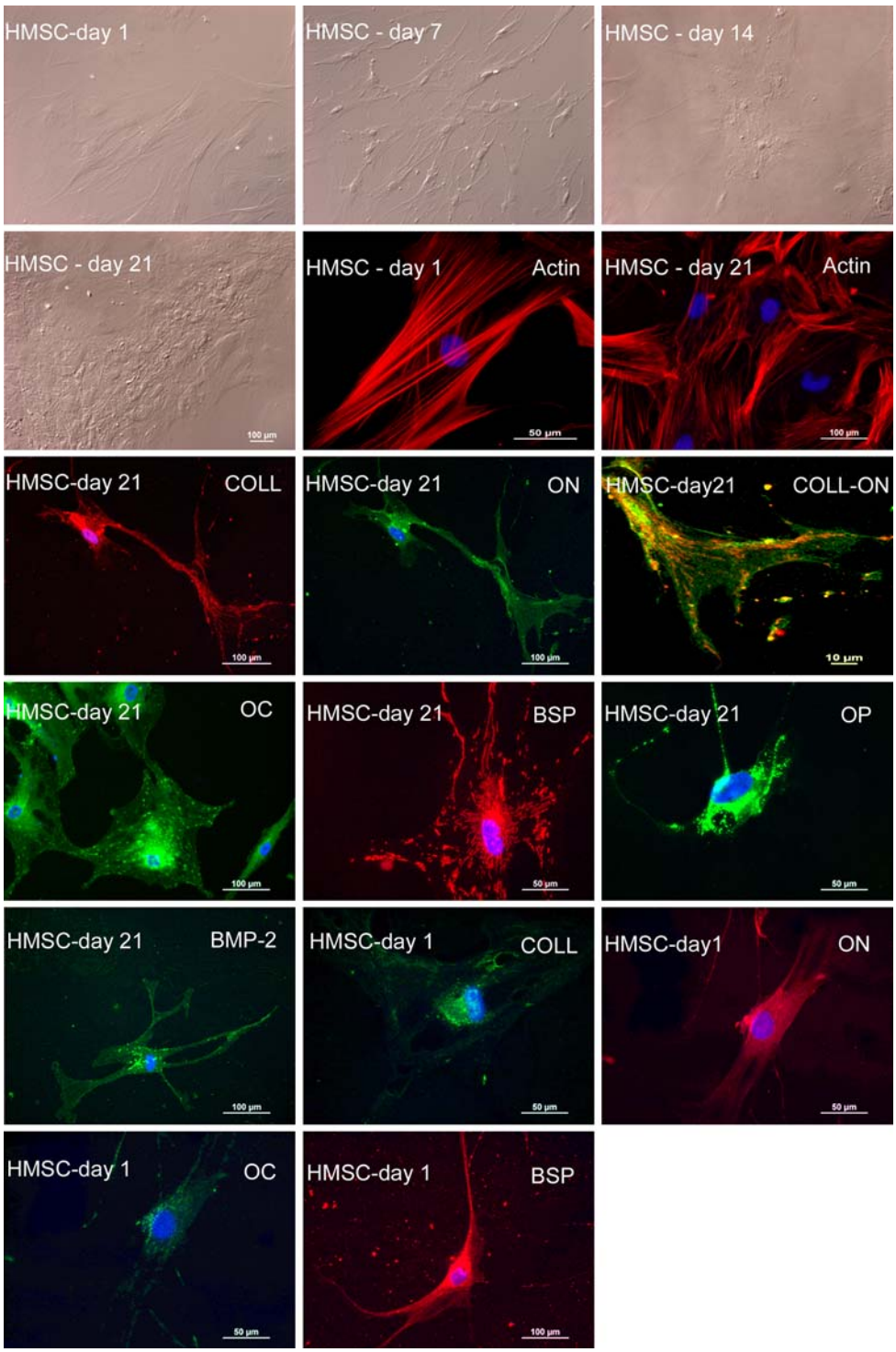

Fig. 1 Morphological and immunocytological analysis of primary OBs differentiated from HMSC. HMSC were grown in differentiation medium for 21 days (see Sect. 2); cell morphology was analyzed with DIC filter (day 1, 7,14 and 21) (bar = 100 μm); actin pattern and expression of OB phenotype markers collagen type I (COLL), osteopontin (OP), osteocalcin (OC), bone sialoprotein (BSP) bone morphogenetic protein-2 (BMP-2) in HMSC (day 1 and 21) were analyzed by immunofluorescence microscopy

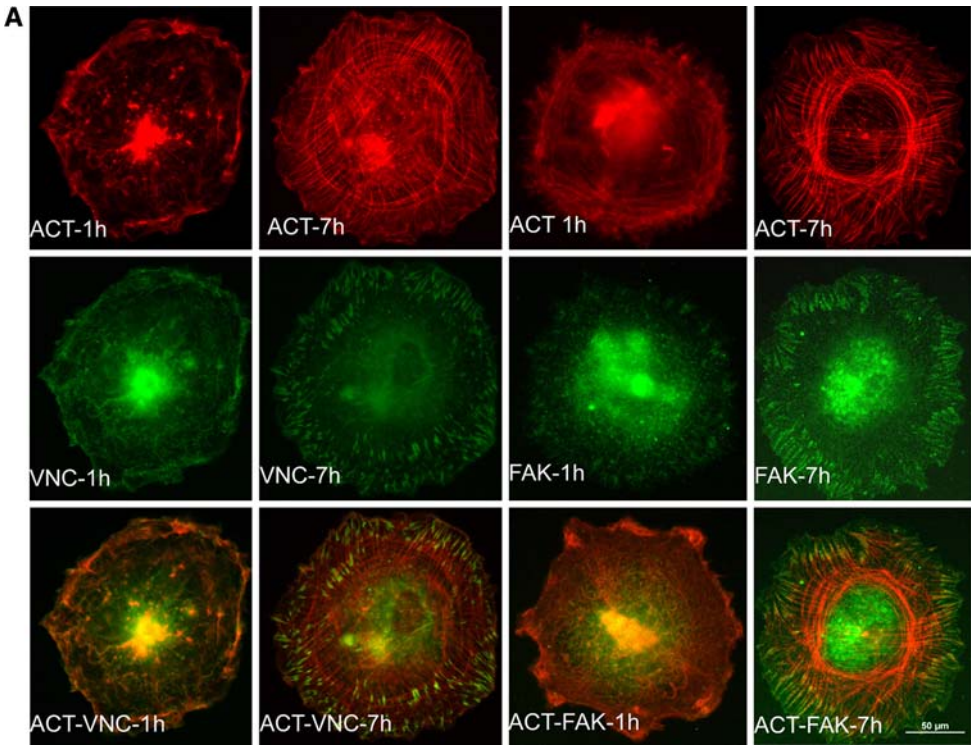

Fig. 2 Adhesion and proliferation of primary OBs onto Ti coated with HA–MP nanohybrids. **A** OBs grown in standard conditions for 1 h and 7 h (bar = 50 µm); (**B** and **C**) OBs grown on Ti coated with HA (**B** a–c), MP (**B** d–f) or HA–MP (**B** g–l). All cells were immunoprobed for actin-ACT (**B**, a, d, g, j and **C**, a, d, g), vinculin-VNC (**B**, b, e, h, k) and Focal Adhesion kinase-FAK (**C**, b, e, h) (bar = 20 µm for **B**, a, b, c; bar = 50 µm for **B**, d–l; **C**, a–c; bar = 100 µm for **C**, Ki67/actin) (see Sect. 2) and analyzed by fluorescence microscopy

several gene products well acknowledged as OB markers was further analyzed in HMSC day 21 and day 1 and results are presented in Fig. 1. At day 21 long fibrils positive for type I collagen and fine punctate vesicles positive for osteonectin appeared in the cytoplasm. Both collagen and osteonectin staining were detected in an extended area of cell body far from nucleus where they partially overlap (Fig. 1, HMSC day21 COLL-ON). The osteopontin and bone sialoprotein were detected in both cytoplasm and in plasma membrane vicinity in bright fluorescent substructures indicating that these proteins had high expression levels. Large granules positive for osteocalcin and bone morphogenetic protein-2 were concentrated in perinuclear area and also along filamentous structures suggesting they were engaged in the secretory process. All markers discussed above were present but poorly expressed in HMSC day 1. The results of this analysis demonstrated that HMSC delineated to osteogenic phenotype within 21 days in differentiation medium. HMSC day 21 were further referred to as primary osteoblasts (OBs) and used in the experiments with biomaterials described in Sect. 2.1.

3.2 Expression of adhesion and proliferation markers in OBs grown on composites-coated Ti

In order to discriminate between Ti–HA, Ti–MP and Ti–HA–MP in relation with their properties to induce OB adhesion we first defined the characteristics (morphology and subcellular distribution) of cytoskeleton (actin-ACT) and other adhesion markers (Vinculin-VNC and Focal adhesion kinase-FAK) during the OBs adhesion on standard cover glass materials (CG) as surface-model. VNC is a membrane cytoskeletal protein in focal adhesion plaques that is involved in linkage of integrin adhesion molecules to the actin cytoskeleton. VNC is associated with cell–cell and cell–extracellular matrix adherens type junctions, being involved in anchoring F-actin to the membrane [40]. FAK is a cytoplasmic tyrosine kinase which colocalizes with integrins in focal adhesions [41]. Five thousand OBs were grown in standard conditions for 1 or 7 h and dynamics of cytoskeleton and subcellular distribution of adhesion markers were observed by immunofluorescence microscopy (Fig. 2A). Within 1 h ACT, VNC and FAK were poorly expressed. ACT was localized at plasma membrane and revealed an irregular, wavy cell contour. VNC and FAK were concentrated in perinuclear areas or diffusely in cytoplasm. After 7 h long ACT filaments traversed entire cell body; VNC and FAK were clearly concentrated in spindle or triangled shaped substructures at plasma membrane or under it where colocalized with ACT termini and no changes in these parameters were observed after 7 h. Based on these observations we evaluated as *poorly adhered OBs* cells having the characteristics described for OBs grown on CG for 1 h, and *fully adhered OBs* the cells having the characteristics described for OBs grown on CG for 7 h.

Next, OBs cultured for 72 h on biomaterials were analyzed for the adhesion markers (Fig. 2B). This time period

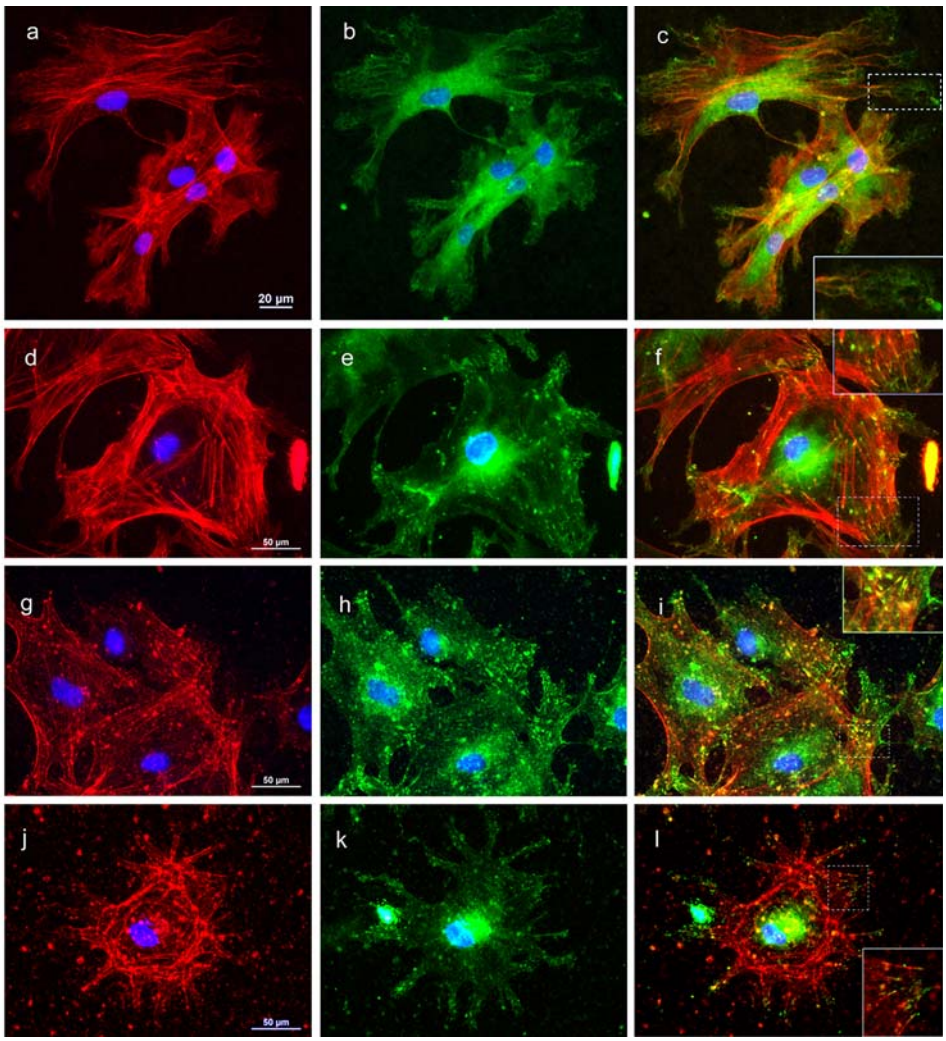

Fig. 2 continued

was selected to detect proliferative cells, if any. In OBs grown on Ti–HA the ACT filaments were very thin and wavy and did not stretch in cell periphery (Fig. 2B, a and c inset). The staining for VNC was very poor in cell extremities and no spindle-shaped VNC positive structures were detected (Fig. 2B, b). OBs grown on Ti coated with HA for 72 h had common characteristics with cells grown in standards conditions for 1 h, suggesting their poor adhesion to this substrate.

In OBs grown on Ti–MP (Fig. 2B, d–f) and Ti–HA–MP (Fig. 2B g–l) ACT fibers appeared as basket-type (Fig. 2B, d, g, j) and spike-like structures of VNC colocalized with actin termini (Fig. 2B, f, i, l insets), which indicate that firm contact points between cells and biomaterial surface have been established. In OBs grown on both Ti–HA (Fig. 2C, b) and Ti–MP (Fig. 2C, e), FAK was poorly expressed and remained localized diffusely in perinuclear area whereas in OBs grown on Ti–HA–MP (Fig. 2C, h) FAK positive granules were visible in a distal position from nucleus suggesting FAK trafficking to cell periphery. Next, OBs grown on biomaterials were further tested for the expression of the proliferation marker protein Ki67. Ki67 is a nuclear antigen expressed in cells in late G1, S, G2 and M phases but not in cells in G0 phase (resting cells) [42]. In Fig. 2C (lower panel) Ki67 positive OBs grown on Ti–HA–MP were shown by arrows; from a total number of eight DAPI positive cells (Fig. 2C, j) five cells were Ki67 positive (Fig. 2C, k). Ki67 positive cells were also detected on Ti coated with HA or MP only (data not shown).

3.3 Specific phenotype and controlled proliferation rate of OBs cultured on Ti–HA–MP

In order to obtain a better evaluation of HA–MP coatings comparatively with HA or MP regarding their properties to regulate specifically bone cell physiology, we analyzed the expression of OB phenotype specific markers on cells grown on composites-coated Ti (Fig. 3). In cells cultured on Ti–MP and Ti–HA–MP immunofluorescence for collagen was intense and appeared as long thin filaments

Fig. 2 continued

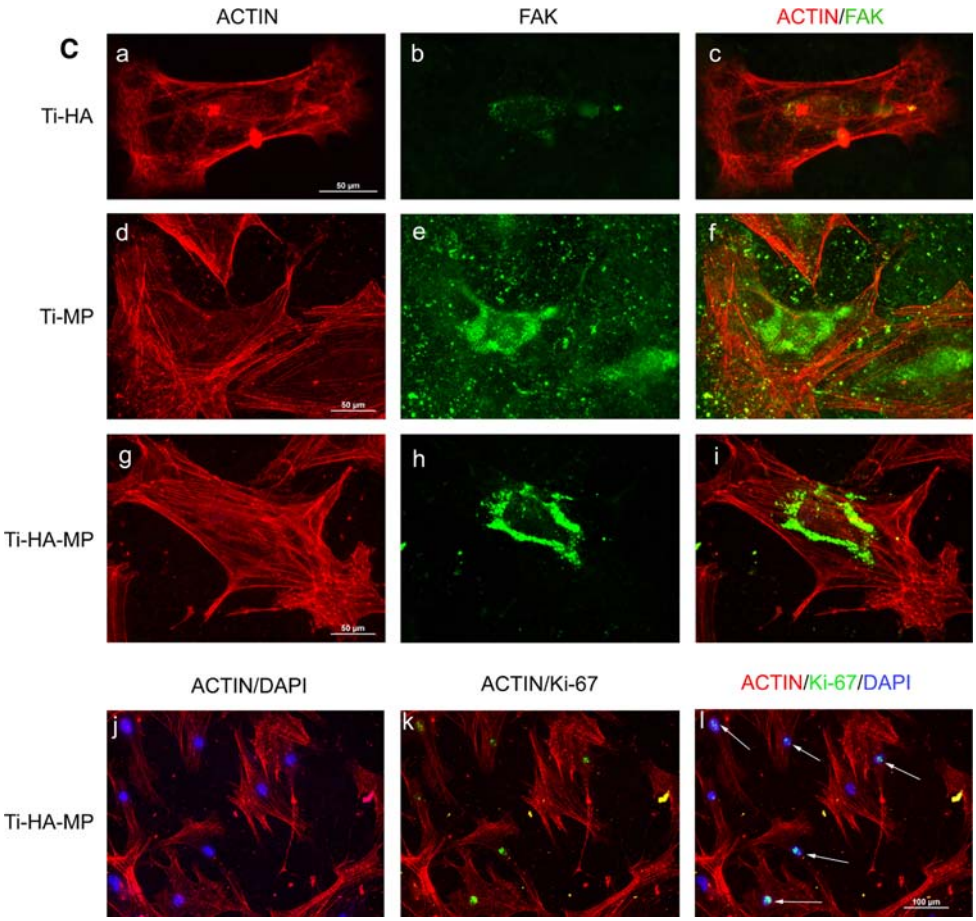

(Fig. 3b, c-insets) traversing the cell body whereas in cells grown on Ti–HA collagen staining was punctuate and concentrated around nucleus (Fig. 3a-inset, see arrow). In cells grown on all three types of coatings bone sialoprotein was well expressed and localized in vesicles in Ti–HA (Fig. 3d) or in filamentous structures in Ti–MP and Ti–HA–MP (Fig. 3e, f). Cells cultured on Ti–HA poorly expressed osteopontin (Fig. 3j) and osteonectin (Fig. 3g); in OBs grown on Ti–MP osteonectin was concentrated in perinuclear area whereas in OBs grown on Ti–HA–MP both osteonectin and osteopontin were more dispersed in cytoplasmic structures. Important to note that in OBs grown on Ti–HA (COLL or OP staining) a portion of the cell body (shown by arrow in Fig. 3) is visibly detached indicating these cells weakly adhered to the surface coated with HA.

As Ki67 positive OBs detected on Ti coated surfaces represented an indicative of proliferative activity, cell proliferation was further quantitatively assessed by CFSE test. CFSE enters cells as CFDA SE (carboxyfluorescein diacetate succinimidyl ester), a non polar molecule that spontaneously penetrates cell membranes and is converted to anionic CFSE by intracellular esterases. CFSE spontaneously and irreversibly couples to proteins by reaction with available amine groups resulting in a stable long-term intracellular retention. With each cell division, fluorescently labeled proteins are equally distributed between daughter cells, which therefore become half as fluorescent as parental cells. Hence, CFSE-high cells have no or low proliferative activity whereas CFSE-low cells have undergone several cell divisions. CFSE-labelled OBs were seeded onto biomaterial or standard surfaces and analyzed by flow cytometry after 6 days in culture. CFSE fluorescence intensity was assessed on a logarithmic scale on the FL-1 channel. In histograms presented in Fig. 4 the population of CFSE-low and CFSE-high OBs were indicated as peak M1 and peak M2, respectively. The percentage of cells in each of the two populations were determined from histogram statistics and represented as bar diagram of averaged duplicates (Fig. 4, lower panel). These data showed that Ti coated with HA or MP generated a higher proportion of CFSElow OBs (50 and 60%, respectively) than Ti coated with HA–MP and control (40%), which indicates an increased frequency of cell divisions during the 6 days in culture on HA or MP coatings.

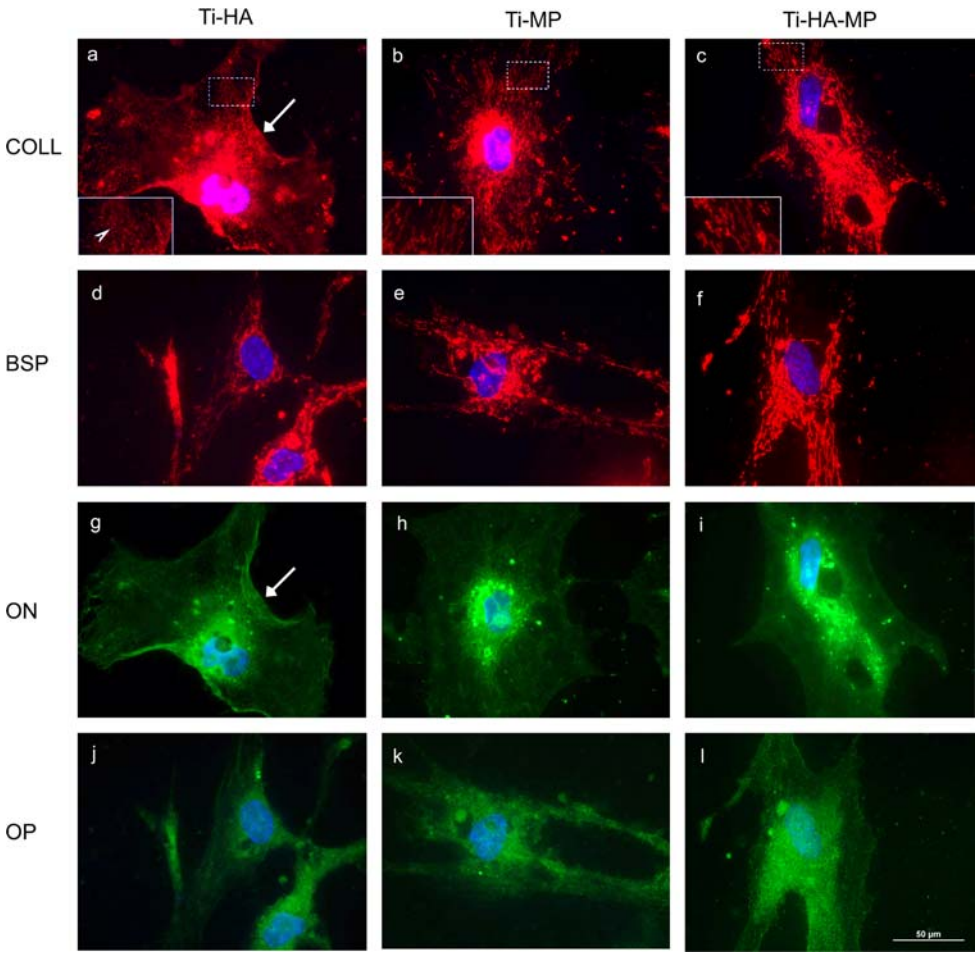

Fig. 3 The expression of osteoblast specific phenotype markers in OBs cultured on Ti coated with HA, MP or HA–MP. OBs grown on the indicated biomaterials immunostained for collagen type I (COLL), bone sialoprotein (BSP), osteonectin (ON) and osteopontin (OP) (bar = 50 µm) (see Experimental Sect. 2.3)

4 Discussion

The interaction of cells with extracellular environment is critical for their proper functioning. Extracellular matrices do not represent only the mechanical anchorage support but the milieu which modulates cell–cell communications or intracellular processes. In reconstituted systems, as biological implants are, cell activities or differentiation pathways can be conducted as well by biomaterial composition and structure. Most biomaterial coatings used in bone implantology contain HA functionalized with various components as amino acids [43], peptides [44], proteins [45] or (bio)polymers [46, 47] in order to improve bone cell adhesion onto these structures. In addition to chemical composition surface morphology represents another important factor which controls cell metabolism on reconstituted structures.

The recently introduced combination between HA and sodium maleate copolymer (MP) obtained by hydrothermal synthesis demonstrated the nanometric structure of the hybrid compounds and their deposition on Ti surfaces by MAPLE technique generated a coating surface with specific characteristics.

To explore the biological properties of Ti surfaces coated with HA–MP nanohybrids, proposed for dental implantology, bone-derived cells were required. Many studies report that adult stem cells can differentiate into osteoblastic lineage in the presence of specific factors [48, 49]. Therefore, in order to use a pool of OBs with similar characteristics in all experiments, a standardized procedure which allowed obtaining of primary OB from HMSC was established in our laboratory. The comparative analysis of cell morphology and expression of OB specific markers during differentiation period validated the osteoblast cell phenotype. Within approximately 21 days in osteogenic medium, HMSC from bone marrow delineated to OBs and became highly positive for type I collagen, osteonectin, osteopontin, bone sialoprotein and bone morphogenetic protein-2 (Fig. 1).

One important parameter to evaluate the surface biocompatibility of the biomaterials destined to be orthopedic or dental implants is cell adhesion. Beyond mechanical anchorage, the adhesion of cells to substrates activates signal transduction pathways which trigger and modulate different gene expression with synthesis of specific proteins and eventually proliferation [50]. The firm cell adhesion

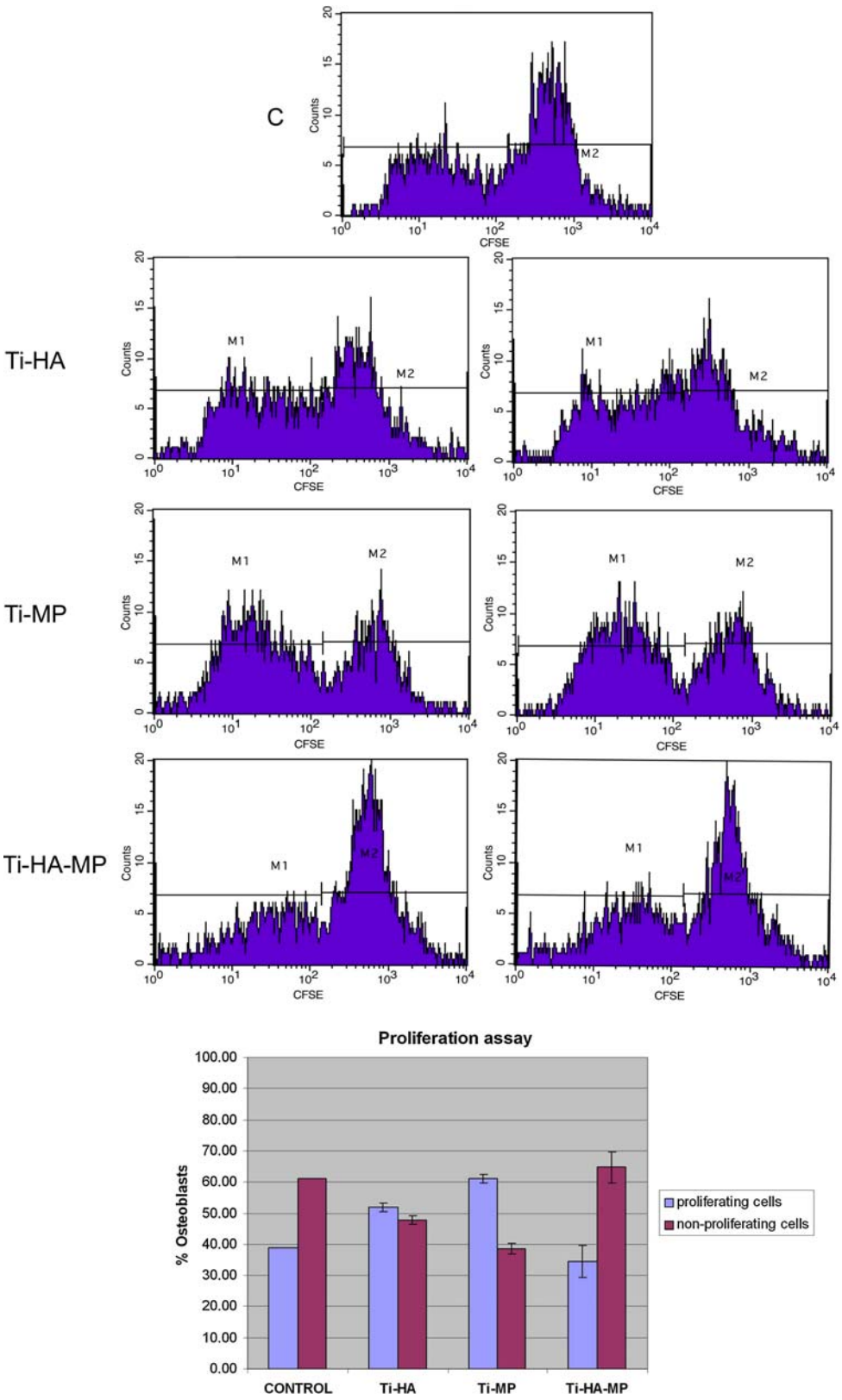

Fig. 4 Proliferation of human OBs grown on Ti coated with HA–MP biomaterials. OBs were labeled with CFSE reagent and cultured for 6 days on standard materials (control-C) or on the indicated biomaterials and analyzed by flow cytometry (see Experimental Sect. 2.4)

and activation of signaling pathways depend on cell phenotype [51, 52] and surface properties [53, 54]. Therefore, dynamics of cell morphology and cytoskeleton as well as subcellular distribution of adhesion markers were analyzed in OBs grown in standard conditions comparatively with OBs cultured on Ti coated surfaces. According to these

data we scored as poorly adhered the OBs having irregular cell contour, ACT localization at plasma membrane, VNC and FAK concentrated in nuclear area (Fig. 2a, ACT-VNC-1 h; ACT-FAK, 1 h). Fully adhered OBs were characterized by the *basket-type* of ACT staining and redistribution of immunoreactivity for VNC and FAK in cell periphery (Fig. 2a, ACT-VNC, 7 h; ACT-FAK, 7 h). OBs cultured on different coated surfaces demonstrated distinct expression and localization patterns of the above analyzed markers (Fig. 2B). OBs grown on Ti–MP and Ti–HA–MP had an ordered ACT network and triangled–shaped VNC staining, clearly indicating cell anchorages to the biomaterial surface (Fig. 2B, f, l, l-insets). The altered morphology of cytoskeleton and VNC localization of OBs cultured on Ti–HA (Fig. 2B, c-inset) demonstrated their poor adhesion to this substrate. In OBs grown on Ti–HA cytoskeleton reorganizes in very thin and wavy acting filaments. Cell nuclei were smaller than in OBs grown on MP or HA–MP coated Ti or control surfaces and VNC appeared also as long filaments decorating the contour of many vacuolar structures. Interestingly, the intense staining of FAK and VNC found in adhesion plaques of OBs grown in standard conditions was not detected in cells grown on any of these biomaterials (Fig. 2a). The different intensities in FAK immunostaining in OBs grown on the three coatings demonstrated that FAK expression was modulated by the biomaterial surface properties and was enhanced by Ti coating with HA–MP only. As FAK is a protein that requires interaction of integrins with ECM for its expression [55] we can speculate that OBs established stronger interactions with ECM via integrins when were cultured on Ti–HA–MP than on the other two coatings.

The data obtained from the analysis of the expression of OB phenotype markers showed that in OBs grown on Ti coated with HA collagen did not assemble into fibrils and osteopontin and osteonectin were detected mainly in the perinuclear area (Fig. 3). The alterations observed in the assembly and traffic of the specific biosynthetic compounds of OBs grown on Ti–HA could represent the consequences of the fact that OBs poorly adhered onto this substrate. However, OBs grown on Ti–HA were proliferative and would generate progenies with distinct morphological and functional characteristics from normal cells. An explanation for such behavior of cells in contact with HA, which otherwise is a largely used ceramic for coating, could be related to the deposition method. As MAPLE is more suitable for transferring polymers than inorganic compounds, Ti coating with HA by MAPLE probably generated a less biocompatible coating structure than HA–MP nanohybrids.

According to the data acquired from quantitative proliferation assay OBs following culture on Ti–MP surfaces underwent through significantly increased number of cell cycles than cells grown on Ti–HA–MP (Fig. 4). This result was in agreement with our previous report which showed increased proliferation of HEK cells on Ti–HA–MP compared to Ti–HA only [37] and supports the idea that polymer could have mitogenic properties. However, OBs are cells with slow growth and multiplication [49]. Their enhanced proliferation following culture on Ti–MP coating could affect gene expression and subsequently induce alterations in the synthesis of bone ECM components. The effects of MP on different cell processes are insufficient understood at this time; however, its lack of cytotoxicity and ability to induce cell adhesion and proliferation recommend MP as an interesting candidate in designing new biocompatible structures.

All together the data presented in this study demonstrated that nanohybrid structures resulted from association of HA with MP copolymer and its deposition on metallic surfaces by MAPLE technique generated a more contributive environment than HA or MP alone, on which OBs firmly adhered, synthesized organic components of their natural ECM and underwent controlled proliferation.

5 Conclusions

The newly developed nanohybrid structures consisting of hydroxyapatite (HA) and sodium maleate-vinyl acetate copolymer (MP) deposited on Ti surfaces proposed for bone implantology were evaluated for their properties related to viability and functionality of bone derived cells. Osteoblasts obtained from bone marrow mesenchymal stem cells were cultured in contact with the Ti coated with HA, MP or HA–MP nanohybrids and analyzed for cell morphology, adhesion as well as for the expression and subcellular localization of the specific markers of osteoblast phenotype and proliferation. Overall results indicated that HA–MP coating represents a structure well tolerated by bone cells. OBs firmly adhered to this surface, synthesized protein components of the ECM and underwent several proliferation cycles. Further studies regarding the effect of Ti coated with HA–MP in bone tissue formation/regeneration are expected to be developed in vivo on animal models.

Acknowledgments This work was supported by National Program Research for Excellence Grant no. 46/2005-2008. The authors thank to Dr. Roxana Mustata for contribution to the preparation of fluorescence microscopy figures and to Emilia Ardelean for technical assistance.

References

1. Implantable medical devices and biocompatible materials industry (Review), Business Communications Company, Inc. USA; 2000.

2. Schmalz G. Concepts in biocompatibility testing of dental restorative materials. Clin Oral Invest. 1998;1:154–62.
3. Kirkpatrick CJ, Peters K, Hermanns MI, Bittinger F, Krump-Kovalinkova V, Fuchs S, Unger RE. In vitro methodologies to evaluate biocompatibility : status quo and perspective. ITBM-RBM. 2005;26:192–9.
4. Black J. Biological performance of materials: fundamentals of biocompatibility. USA: CRC Press; 2006.
5. Kirkpatrick CJ, Mittermayer C. Theoretical and practical aspects of testing potential biomaterials in vitro. J Mater Sci: Mater Med. 1990;1:9–13.
6. Allen MJ, Rushton N. Use of the CytoTox 96 assay in routine biocompatibility testing in vitro. Promega Notes. 1994;45:7–10.
7. Jäger M, Fischer J, Schultheis A, Lensing-Höhn S, Krauspe R. Extensive H(+) release by bone substitutes affects biocompatibility in vitro testing. J Biomed Mater Res. 2006;76:310–22.
8. Van Kooten TG, Klein CL, Kohler H, Kirkpatrick CJ, Williams DF, Eloy R. From cytotoxicity to biocompatibility testing in vitro: cell adhesion molecule expression defines a new set of parameters. J Mater Sci: Mater Med. 1997;8:835–41.
9. Locci P, Marinucci L, Lilli C, Belcastro S, Staffolani N, Bellocchio S, et al. Biocompatibility of alloys used in orthodontics evaluated by cell culture tests. J Biomed Mater Res. 2000;51:561–8.
10. Suh H, Park JC, Han D-W, Lee DH, Han CD. A bone replaceable artificial bone substitute: cytotoxicity, cell adhesion, proliferation, and alkaline phosphatase activity. Artif Organs. 2001;25:14–21.
11. Hailea Y, Haasterta K, Cesnuleviciusa K, Stummeyerb K, Timmera M, Berskic S, et al. Culturing of glial and neuronal cells on polysialic acid. Biomaterials. 2007;28:1163–73.
12. Ribeiro D, Duarte M, Matsumoto M, Marques M, Salvadori D. Biocompatibility in vitro tests of mineral trioxide aggregate and regular and white portland cements. J Endod. 2005;31:605–7.
13. Braz MG, Camargo EA, Salvadori DMF, Marques MEA, Ribeiro DA. Evaluation of genetic damage in human peripheral lymphocytes exposed to mineral trioxide aggregate and Portland cements. J Oral Rehabil. 2006;33:234–9.
14. Shida J, Trindade MC, Goodman SB, Schurman DJ, Smith RL. Induction of interleukin-6 release in human osteoblast-like cells exposed to titanium particles in vitro. Calcif Tissue Int. 2000; 67:151–5.
15. Vahey JW, Simonian PT, Conrad EU. Carcinogenicity and metallic implants. Am J Orthop. 1995;24:319–24.
16. Trindade MCD, Lind M, Nakashima Y, Sun D, Goodman SB, Schurman DJ, et al. Interleukin-10 inhibits polymethylmethacrylate particle induced interleukin-6 and tumor necrosis factor-alpha release by human monocyte/macrophages in vitro. Biomaterials. 2001;22:2067–73.
17. Keselowsky BG, Collard DM, Garcia AJ. Integrin binding specificity regulates biomaterial surface chemistry effects on cell differentiation. Proc Natl Acad Sci USA. 2007;102:5953–7.
18. Jacobs JJ, Gilbert JL, Urban RM. Corrosion of metal orthopaedic implants. J Bone Joint Surg Am. 1998;80:268–82.
19. Staffolani N, Damiani F, Lilli C, Guerra M, Staffolani NJ, Belcastro S, et al. Ion release from orthodontic appliances. J Dent. 1999;27:449–53.
20. Le MK, Zhu XM. In vitro corrosion resistance of plasma source ion nitrided austenitic stainless steels. Biomaterials. 2001;22: 641–7.
21. Cui ZD, Chen MF, Zhang LY, Hu RX, Zhu SL, Yang XJ. Improving biocompatibility of NiTi alloy by chemical treatments: an in vitro evaluation in 3T3 human fibroblast cells. Mater Sci Eng C. 2008;28:1117–22.
22. Ben-Nissan B, Milev A, Vagoc R. Morphology of sol–gel derived nano-coated coralline hydroxyapatite. Biomaterials. 2004;25: 4971–5.
23. Kim H-W, Kim H-E. Nanofiber generation of hydroxyapatite and fluor-hydroxyapatite bioceramics. J Biomed Mater Res B Appl Biomaterials. 2005;77b:323–328.
24. Wang Y-W, Wu Q, Chen J, Chen G-Q. Evaluation of three-dimensional scaffolds made of blends of hydroxyapatite and poly(3-hydroxybutyrate-co-3-hydroxyhexanoate) for bone reconstruction. Biomaterials. 2005;26:899–904.
25. Bishop A, Balazsi C, Yang JHC, Gouma P-I. Biopolymer-hydroxyapatite composite coatings prepared by electrospinning. Polym Adv Technol. 2006;17:902–6.
26. Kumar R, Prakash KH, Cheang P, Gower L, Khor KA. Chitosan-mediated crystallization and assembly of hydroxyapatite nanoparticles into hybrid nanostructured films. J R Soc Interface. 2008;5:427–39.
27. Pique A. Deposition of polymers and biomaterials using the matrix-assisted pulsed evaporation (Maple) process. In: Eason R, editor. Pulsed laser deposition of thin films. Applications-led growth of functional materials. Hoboken, NJ: Wiley-Interscience; 2007.
28. Cristescu R, Mihailescu IN, Jelinek M, Chrisey DB. Functionalized thin films and structures obtained by novel laser processing issues. In: Kassing R, Petkov P, Kulisch W and Popov C, editors. Functionalized properties of nanostructured materials, Nato Science Series II: Mathematics, Physics and Chemistry, Vol. 223. Springer, 2006. p. 211.
29. Frycek R, Jelinek M, Kokourek T, et al. Thin organic layers prepared by MAPLE for gas sensor application. Thin Solid Films. 2006;495:308–11.
30. Jelinek M, Cristescu R, Mihailescu IN, Chrisey DB, et al. Matrix assisted pulsed laser evaporation of cinnamate-pullulan and tosylate-pullulan polysaccharide derivative thin films for pharmaceutical applications. Appl Surf Sci. 2007;253:7755–60.
31. Gyorgy E, Axente E, Mihailescu IN, Predoi D, Ciuca S, Neamtu J. Creatinine biomaterial thin films grown by laser techniques. J Mater Sci. 2008;19:1335–9.
32. Cristescu R, Mihailescu IN, Stamatin I, Doraiswamy A, Narayan RJ, Westwood G, et al. Thin films of polymer mimics of cross-linking mussel adhesive proteins deposited by matrix assisted pulsed laser evaporation. Appl Surf Sci. 2009;255:5496–8.
33. Klepetsanis KP, Koutsoukos PG, Chitanu GC, Carpov A. Application of water soluble polymers. In: Amjad Z, editors. Acs Symposium Series, New York; 1998. p. 117.
34. Bouropoulos K, Bouropoulos N, Melekos M, Koutsoukos PG, Chitanu GC, Anghelescu-Dogaru AG, et al. The inhibition of calcium oxalate monohydrate crystal growth by maleic acid copolymers. J Urol. 1998;159:1755–61.
35. Piticescu RM, Chitanu GC, Popescu ML, Lojkowski W, Opalinska A, Strachowski T. New hydroxyapatite based nanomaterials for potential use in medicine. Ann Transpl. 2004;9:20–5.
36. Piticescu RM, Chitanu GC, Albulescu M, Giurginca M, Popescu ML, Lojkowski W. Hybrid HAp-maleic anhydride copolymer nanocomposites obtained by in situ functionalisation. Solid State Phenomena. 2005;106:47–56.
37. Negroiu G, Piticescu RM, Chitanu GC, Mihailescu IN, Zdrentu L, Miroiu M. Biocompatibility evaluation of a novel hydroxyapatite-polymer coating for medical implants (in vitro tests). J Mater Sci. 2008;19:1537–44.
38. Chitanu GC, Popescu I, Carpov A. Synthesis and characterisation of maleic anhidryde copolimer and their derivatives. Addition polimerization-literature survey. Rev Roum Chim. 2005;50:589–99.
39. Chitanu GC, Popescu I, Carpov A. Synthesis and characterization of maleic anhydridecopolymers and their derivatives. New data on the copolymerization of maleic anhydride with vinyl acetate. Rev Roum Chim. 2006;51:915–29.
40. Saunders RM, Holt MR, Jennings L, Sutton DH, Barsukov IL, Bobkov A, et al. Role of vinculin in regulating focal adhesion turnover. J Cell Biol. 2006;85:487–500.

41. Lim JY, Dreiss AD, Zhiyi Z, Hansen JC, Siedlecki CA, Hengstebeck RW, et al. The regulation of integrin-mediated osteoblast focal adhesion and focal adhesion kinase expression by nanoscale topography. Biomaterials. 2007;28:1787–97.
42. Scholzen T, Gerde J. The Ki-67 protein: from the known and the unknown. J Cell Physiol. 2000;182:311–22.
43. Gonzalez-Mcquire R, Chane-Ching J-Y, Vignaud E, Lebugle A, Mann S. Synthesis and characterization of amino acid-functionalized hydroxyapatite nanorods. J Mater Chem. 2004;14:2277–81.
44. Hennessy KM, Pollot BE, Clem WC, Phipps MC, Sawyer AA, Culpepper BK, et al. The effect of collagen I mimetic peptides on mesenchymal stem cell adhesion and differentiation, and on bone formation at hydroxyapatite surfaces. Biomaterials. 2009;30:1898–909.
45. Murphy MB, Hartgerink JD, Goepferich A, Mikos AG. Synthesis and in vitro hydroxyapatite binding of peptides conjugated to calcium-binding moieties. Biomacromolecules. 2007;8:2237–43.
46. Suratwala SJ, Cho SK, Van Raalte JJ, Park SH, Seo SW, Chang SS, et al. Enhancement of periprosthetic bone quality with topical hydroxyapatite-bisphosphonate composite. J Bone Joint Surg Am. 2008;90:2189–96.
47. Schneiders W, Reinstorf A, Biewener A, Serra A, Grass R, Kinscher M, et al. In vivo effects of modification of hydroxyapatite/collagen composites with and without chondroitin sulphate on bone remodeling in the sheep tibia. J Orthop Res. 2009;27:15–21.
48. Bianco P, Riminucci M, Gronthos S, Robey PG. Bone marrow stromal stem cells: nature, biology, and potential applications. Stem Cells. 2001;19:180–92.
49. Buttery LD, Bourne S, Xynos JD, Wood H, Hughes FJ, Hughes SP, et al. Differentiation of osteoblasts and in vitro bone formation from murine embryonic stem cells. Tissue Eng. 2001;7:89–99.
50. Juliano RL. Signal transduction by cell adhesion receptors and the cytoskeleton: functions of integrins, cadherins, selectins, and immunoglobulin-superfamily members. Ann Rev Pharmacol Toxicol. 2002;49:283–323.
51. Lampin M, Warareocquier-Clerout R, Legris C, Degrange M, Sigot-Luizard MF. Correlation between substratum roughness and wettability, cell adhesion, and cell migration. J Biomed Mater Res. 1997;36:99–108 .
52. Anselme K. Osteoblast adhesion on biomaterials. Biomaterials. 2000;21:667–81.
53. Keselowsky BG, Collard DM, Garcia AJ. Surface chemistry modulates focal adhesion composition and signaling through changes in integrin binding. Biomaterials. 2004;25:5947–54.
54. Zreiqat H, Valenzuela SM, Nissan BB, Roest R, Knabe C, Randalski RJ, et al. The effect of surface chemistry modification of titanium alloy on signaling pathways in human osteoblasts. Biomaterials. 2005;26:7579–86.
55. Clark EA, Brugge JS. Integrins and signal transduction pathways: the road taken. Science. 1995;268:233–9.